Pergamon

Chaos, Solitons & Fractals, Vol. 9, No. 3, pp. 377–392, 1998

Printed in Great Britain
0960-0779/98 $19.00 + 0.00

PII: S0960-0779(97)00125-2

Bifurcation-reconnection Sequences in Nonpendular Resonance

G. CORSO

Department of Electrical Engineering and Computer Science, and the Electronics Research Laboratory, University of California, Berkeley, CA 94720, USA

R. PAKTER

Plasma Science and Fusion Center, Massachusetts Institute of Technology, Cambridge, MA 02139, USA

I. L. CALDAS

Instituto de Física, Universidade de São Paulo, Caixa Postal 66318, 05389-970 São Paulo, Brazil

and

F. B. RIZZATO

Instituto de Física, Universidade Federal do Rio Grande do Sul, Caixa Postal 15051, 91501-970 Porto Alegre, Brazil

(Accepted 3 June 1997)

Abstract—In this paper, we show how a whole set of primary resonances can be generated by a definite sequence of bifurcation-reconnections in a nonlinear Hamiltonian system. The resonance generation is accomplished from a sequence of tangent inverse bifurcations followed by reconnection processes inside a nonpendular island nonmonotonic in the frequency. The stability of the nonpendular island is found to be unaffected by these processes except for the [2:1] resonance, where it presents a window of instability. In particular, we consider the problem of particle acceleration in a plasma media and discuss possible implications of the instability window on the acceleration process. © 1998 Elsevier Science Ltd. All rights reserved

1. INTRODUCTION

This paper initially deals with the analysis of sequences of bifurcations that characterize Hamiltonian phase space patterns. We are interested in the analysis of two sequences that originate a complete set of primary resonances in an Hamiltonian system. The main point is that this process is possible because it occurs inside a nonpendular island that is nonmonotonic in the frequency; besides bifurcations there is the presence of reconnections [1, 2] in this system.

The nonpendular resonance is originated in the context of low energy relativistic particle acceleration [3, 4]; one calls this island a nonpendular island, following [5]. One of the most important characteristics of the nonpendular island is the absence of hyperbolic points in its boundary. As a consequence, this resonance island does not develop a stochastic layer in its boundary and follows atypical transition to chaos [6]. The nonpendular island is also found in the restricted three-body problem of celestial mechanics [7].

To carry out this work, we will focus on a physical model from the acceleration context that presents one nonpendular island. Furthermore, the investigation of bifurcation-reconnections process provides a knowledge on stability of island of resonance and by

consequence of the accelerator devices; this is a theme of great technological importance [3, 4, 8, 9].

The paper is therefore organized as follows. In Section 2, we define the physical model and discuss some features related to the nonpendular island; in Section 3, we perform a global analysis of the phase space; in Section 4, we analyze the sequences of bifurcation-reconnections inside the nonpendular island; and in Section 5 we conclude the work.

2. THE MODEL: A NONPENDULAR ISLAND

The model consists of an electron immersed in a background of magnetized plasma which is perturbated by a perpendicular electrostatic wave [6,10]. The wave is characterized by an amplitude A_0, a wave vector k and a frequency ω. The corresponding relativistic Hamiltonian of an electron is written as

$$H = [1 + p_z^2 + (p_x + x)^2 + p_y^2]^{1/2} + A_0 \cos(kx - \omega t), \tag{1}$$

where H is normalized to mc^2, $\mathbf{p}$ to mc, A_0 to e/mc^2, time and space are normalized to $\omega_c = |eB_0/mc|$ and ω_c/c, respectively, with B_0 as the background field, m as the electron mass, c as the velocity of light and e as the electron charge. The injected particle parallel momentum p_z is a constant of motion and can be treated here as a parameter of the system. Although the parameter p_z is a constant of motion, smooth variations of p_z caused by nonhomogenities in the magnetic field are expected.

Using guiding-center variables defined as

$$p_x = \sqrt{2I}\cos\phi, \quad x + p_y = \sqrt{2I}\sin\phi, \tag{2}$$

and making use of the harmonic expansion for Bessel functions J_l, it becomes possible to cast the Hamiltonian in the resonant form

$$H = [1 + 2I + p_z^2]^{1/2} + A_0 \sum_l J_l(k\sqrt{2I})\cos(l\phi - \omega t). \tag{3}$$

This Hamiltonian can be written as $H = H_0 + A_0 H_1$, where $H_0 = \sqrt{1 + 2I + p_z^2}$ is the integrable part of H and $H_1 = \sum_l J_l(k\sqrt{2I})\cos(l\phi - \omega t)$ is its perturbation part. Note that I is directly related to the kinetic energy. All theoretical conclusions from this model are valid even for adiabatic variations of p_z, because the action is an adiabatic invariant.

The natural frequency ω_0 of the system is easily estimated in the action angle coordinates to be

$$\omega_0 = \partial_I H_0 = \frac{1}{\sqrt{1 + 2I + p_z^2}}. \tag{4}$$

As I varies from 0 to ∞, the frequency behaves monotonically. The term H_1 perturbates H_0 giving rise to resonances that are approximated by pendular island whose frequency behaves also monotonically [11]. In this way, one can expect that no reconnections take place in the phase space generated by the Hamiltonian of eqn (3), due to the monotonicity in the frequency. However, the nonpendular island plays a differential role at this point, as we shall see.

2.1 *The resonance condition*

There is a primary resonance $[m,n]$ in the phase space when the resonance condition

$$n\omega_0 = m\omega \tag{5}$$

is fulfilled, where ω_0 is the natural frequency of the system, given by eqn (4), n and m are integers, and ω is an external frequency that perturbates the system [11]. In our case, the perturbing frequency is just the one of the electrostatic wave and the resonances produced are named primary resonances.

Using eqn (5), one can write a resonance condition for the Hamiltonian of eqn (3); this condition assumes the form

$$I_{n,m} = \frac{1}{2}\left(\left(\frac{n}{m\omega}\right)^2 - 1 - p_z^2\right), \tag{6}$$

where $I_{n,m}$ is the value of the action at resonance $[m,n]$. The most important resonances are those where $m=1$; they can be described choosing only one term $l=n$ in the Hamiltonian in eqn (3). We call this the resonance $n=l$, and denote the value of the action at this resonance by I_n.

If one takes a tenuous plasma $\omega=1$ and the resonance $n=1$, the resonance condition in eqn (5) produces a negative value for I_1. However, by eqns (2), I is positive defined; this unusual kind of resonance is known in the literature as a nonpendular island [5].

We can see in eqn (6) that the value of the action in a chosen resonance is a function of the parameter p_z. As p_z increases, I_n brings the n-esim resonance closer to the nonpendular island that is always found in the region of low values of the action I, or low energy. The parameter p_z produces a shift in the position of all resonances. The main aim of this paper is to describe the annihilation of resonances as p_z increase, or, on the other hand, the generation of resonances as p_z decrease.

It is worth saying that the value of the action I_n of many resonances can become negative, but only the resonance $n=1$ will survive becoming a nonpendular island in the region of low energy. This happens because of the larger value of the polynomial representing this island, as compared with others [10].

2.2 *The frequency inside the nonpendular island*

In this paper, we are interested in the process involving a special resonance produced in the low energy regime. To describe its dynamics we choose in eqn (3) the term $n=1$, responsible for acceleration in low energy regime, and discard other terms. After a canonical time removal in the Hamiltonian in eqn (3), one arrives at the local Hamiltonian

$$H_{\text{local}} = [1 + 2I + p_z^2]^{1/2} + A_0 J_1(k\sqrt{2I}) \cos\psi - \omega I, \tag{7}$$

where the new angle coordinate is defined by $\psi = \phi - \omega t$.

The Hamiltonian in eqn (7) describes the nonpendular island. In Fig. 1, we show a contour plot of this Hamiltonian, the parameters used being $\omega = k = 1$, $p_z = 2.3$ and $A_0 = 0.1$. The main aspects of the nonpendular island are pointed out; these are the elliptic point and the island boundary.

We use the Hamiltonian in eqn (7) to estimate the frequency inside the nonpendular island. First we expand the square root and the Bessel function for low values of the action I. The Hamiltonian obtained is

$$H_{\text{local}} = \alpha I + \beta I^2 + \delta\sqrt{I}\cos\psi, \tag{8}$$

where $\alpha \equiv 1/\sqrt{1+p_z^2} - 1$, $\beta \equiv -(1/2)(1+p_z^2)^{-3/2}$ and $\delta \equiv A_0/\sqrt{2}$.

Using the Hamiltonian equations, we can write an effective potential that results

$$\left(\frac{\mathrm{d}I}{\mathrm{d}t}\right)^2 - V(I) = 0 \tag{9}$$

where $V(I) \equiv \delta^2 I - (E - \alpha I - \beta I^2)^2$ and E is the value of the energy.

The integration of eqn (9) produces the period T of the movement

$$T = \frac{\mathrm{d}I}{\sqrt{V(I)}}. \tag{10}$$

where the integration limits coincide with the two real roots of the effective potential V. Finally the frequency $f = 2\pi/T$ can be estimated.

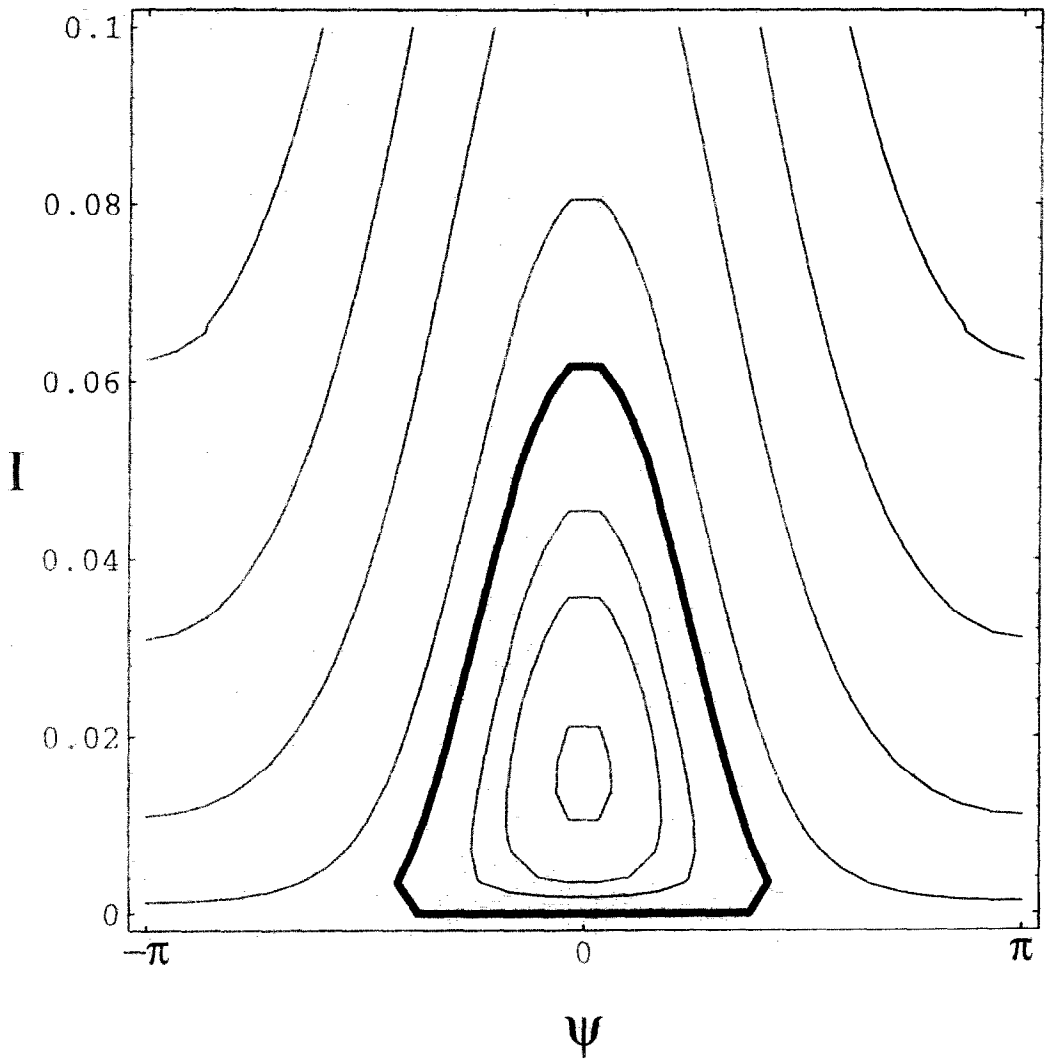

Fig. 1. Sketch of the nonpendular island. On the vertical axis is the variable action and on the horizontal axis the variable angle. The elliptic point of the island and its boundary are indicated.

In Fig. 2, we plot the frequency inside the nonpendular island versus the value of the energy E; the energy of the boundary is indicated. Three curves, corresponding to three values of parallel momentum $p_z = 0.25$, 0.3 and 0.35, are indicated. One observes that the behavior of frequency inside the nonpendular island is nonmonotonic. Moreover, the minimum of frequency drifts as the parameter p_z varies. The situations $p_z = 0$ and $p_z \to \infty$ are two degenerate cases where the extremum drifts, toward the boundary and towards the elliptical point of the nonpendular island, respectively.

3. GLOBAL ANALYSIS OF THE PHASE SPACE

Three issues will be treated in this section. The first is that the nonpendular island allows one to understand all the resonant chains presented in the phase space as generated by bifurcations and reconnections involving itself.

The second is that the generation of resonances corresponds to critical values of p_z. Finally, the third issue deals with the integrable limit of $p_z \to \infty$. In order to explore these points, we will start by analyzing the stability index of the elliptic point of the nonpendular island.

The Newton–Raphson stability algorithm [12] provides the stability index α of a particular periodic orbit. When $|\alpha| > 1$ the corresponding periodic orbit is unstable (one has an unstable fixed point in the Poincaré plots) and when $|\alpha| < 1$ the periodic orbit is stable (one

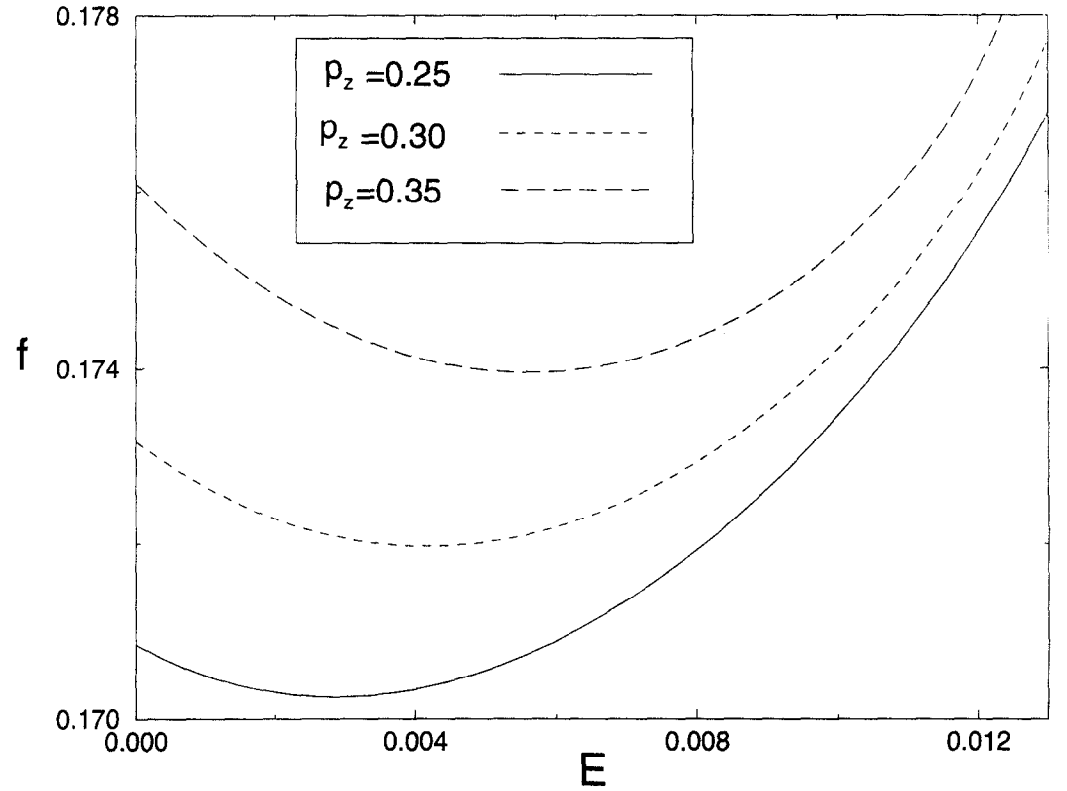

Fig. 2. Analytical estimation for the frequency inside the nonpendular island vs the value of the energy. The scale in energy begins at the elliptic point and ends at the boundary of the island. The three curves correspond to different values of p_z indicated in the figure.

has an elliptic fixed point). For the periodic orbits, the winding numbers can be extracted from the Newton–Raphson algorithm.

The resonance condition for secondary resonances inside the first island is defined by

$$q\omega_{in} = p\omega, \tag{11}$$

where ω_{in} is the frequency of the nonpendular island close to the elliptical point and p and q are integers. The secondary resonance chain has the winding number p/q, where q is the number of islands in the chain. When the winding number assumes a rational value, a secondary resonance appears [11] around this elliptic point. This information is connected with the stability index α by the relation [12]

$$\alpha = \cos 2\pi \frac{p}{q}. \tag{12}$$

In Fig. 3, we can see a diagram of the stability index α versus the longitudinal momentum p_z, for the elliptic point of the nonpendular island, for two values of the amplitude of the wave: (a) $A_0 = 0.05$ and (b) $A_0 = 0.5$. Let us focus our attention on case (a). Two aspects are important: a minimum of the curve and the asymptotic behavior for large p_z. In a detailed simulation, one can see that $\alpha < -1$ at the minimum (see Fig. 7) and so there is a window of instability for the nonpendular island fixed point. This window will be pointed out in the discussion on the sequence of bifurcations during the generation of resonance [2:1].

Using the relation in eqn (12) that provides the secondary resonances present inside the nonpendular island, we indicate in Fig. 3(a) some secondary resonances. Following this picture, the instability of the nonpendular island is simply a situation where $p/q = 1/2$ and a resonance [2:1] is produced. We can see that as p_z increase the number of resonant chains q in the secondary resonances becomes greater; in the asymptotic limit, the nonpendular island produces a resonance with q growing to infinite, and $\alpha \to 1$.

The values of p_z which correspond to the resonances indicated in the Fig. 3(a) are called critical values. Instead of obtaining these values from the relation in eqn (12), we can alternatively use the relation in eqn (6) with $I_{n,m} = 0$. In a experimental situation, these values of p_z are critical because great changes in the phase space can take place and the regular acceleration be destroyed.

In order to get a clearer understanding of the genesis of phase space we are working with, it is better to consider the set of bifurcations generated from the nonpendular island as the parameter p_z decreases from infinite to zero. We define the ring around the elliptic point where the frequency takes an extremum value, and, by consequence, the reconnection process takes place along the reconnection ring. As analyzed in the last section, for $p_z = 0$ the reconnection ring is the nonpendular boundary and as $p_z \to \infty$ the reconnection ring collapses to the elliptic point.

If the frequency behavior of the nonpendular island were monotonic the situation would be easily explained. Each time p_z satisfies eqn (11), a secondary resonance appears in the vicinity of the elliptic point according to a bifurcation well defined by a normal form [13]. As p_z continues to decrease, this resonance migrates to the nonpendular boundary and crosses it becoming a primary resonance. The fact that the frequency inside the nonpendular island is nonmonotonic implies the existence of a reconnection process and the picture above breaks down; in the next section, we will return to this point.

In Fig. 3(b), the situation is characterized by an instability for low values of p_z; the reason is the high amplitude of the wave that chaotize all the phase space. In [14], an appropriate overlapping of resonance criteria is worked out in order to describe the overlapping of resonance between the resonance [2:1] and the nonpendular island.

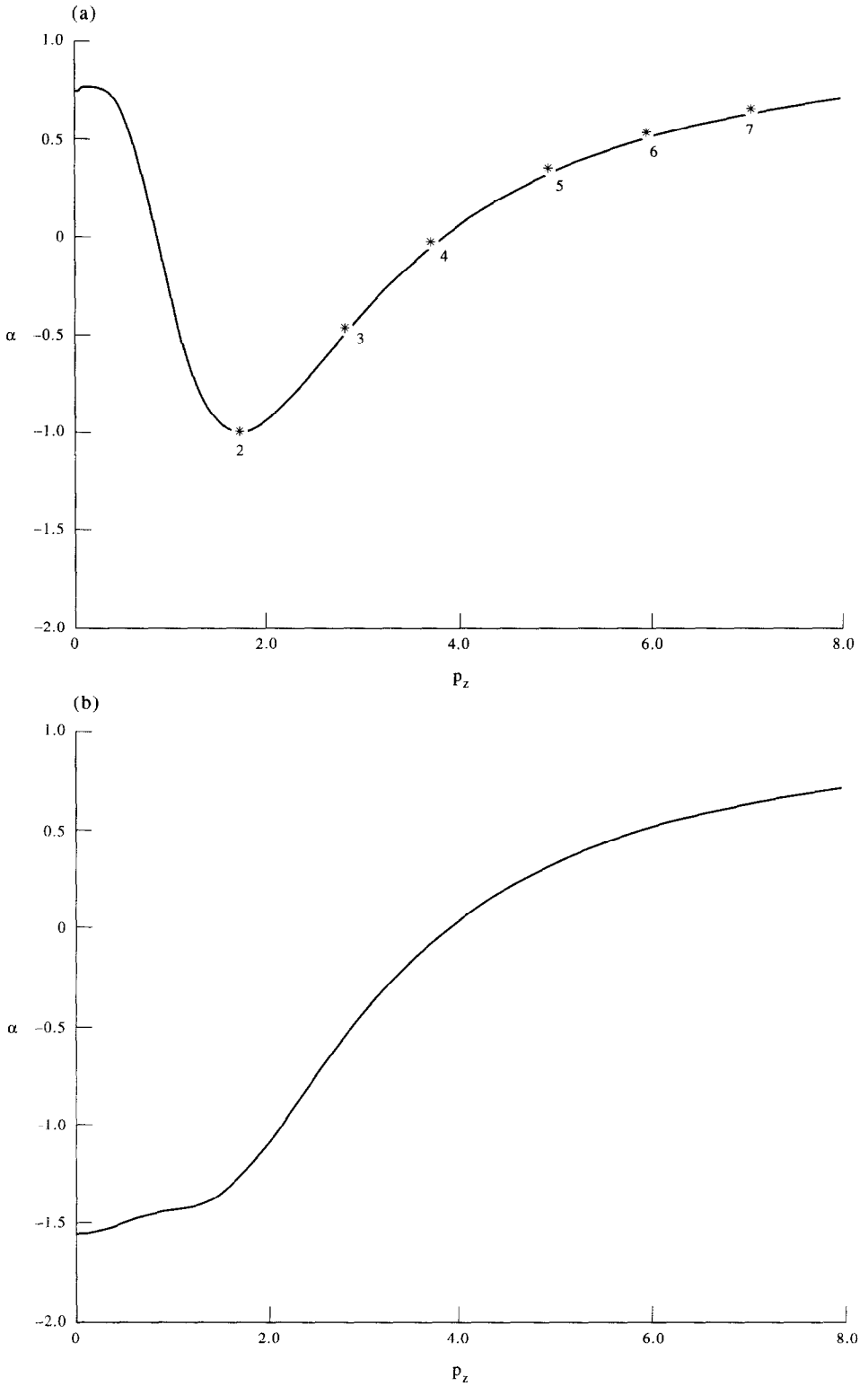

Fig. 3. Stability diagram vs p_z for two values of the amplitude of the wave: (a) $A_0 = 0.05$, (b) $A_0 = 0.5$. In case (a), some values of secondary resonances internal to the nonpendular island are indicated. Here $k = \omega = 1$.

We can see in Fig. 3(a) and (b) that, for large p_z, the stability index α remains always smaller than 1 and, as a consequence, stable. The influence of higher values of p_z compensates for the chaotic dynamics caused by the wave and guides the nonpendular island to stability. Following this picture, p_z can be considered as a chaos suppressing parameter of the system. This aspect can be understood in the context of relativistic dynamics. If one thinks that the relativistic mass of the electron accelerated is done by the γ factor, where $\gamma = H_0$, it is easy to conclude that as p_z becomes larger so will the inertial mass. The stability of the nonpendular island for high p_z can be credited to a high inertial mass of the electron. In the limit $p_z \to \infty$, $H \to H_0$ and the system becomes integrable: this is an alternative way to understand the stability of the system in this limit.

Figure 3(a) can be reproduced analytically from the Hamiltonian of eqn (7) of the nonpendular island. In this way, we will use the resonance condition of eqn (11) for secondary resonances inside the first island. The frequency ω_{in} is obtained in a standard way as in the case of pendular islands [11]. Using the relations of eqns (12) and (11), we reproduce the analytic function of the stability index α versus p_z. In Fig. 4, we can see this figure for the same set of parameters of the simulation showed in Fig. 3(a), just to make possible a comparison. There is a good agreement between the two figures.

There is nevertheless a point where these two figures present a qualitative difference. The theoretic curve in Fig. 4 is tangent to the line $\alpha = -1$, but the simulation curve in Fig. 3(a) crosses $\alpha = -1$ yielding a instability window. As the theoretical estimate do not make use of the other resonances of the system, one can say that the window of instability is due to the nonlinear influence of all other resonances on the nonpendular one. We have made other simulations where a greater amplitude A_0, and consequently greater influence of all the resonances, is taken into account and the window of instability becomes larger.

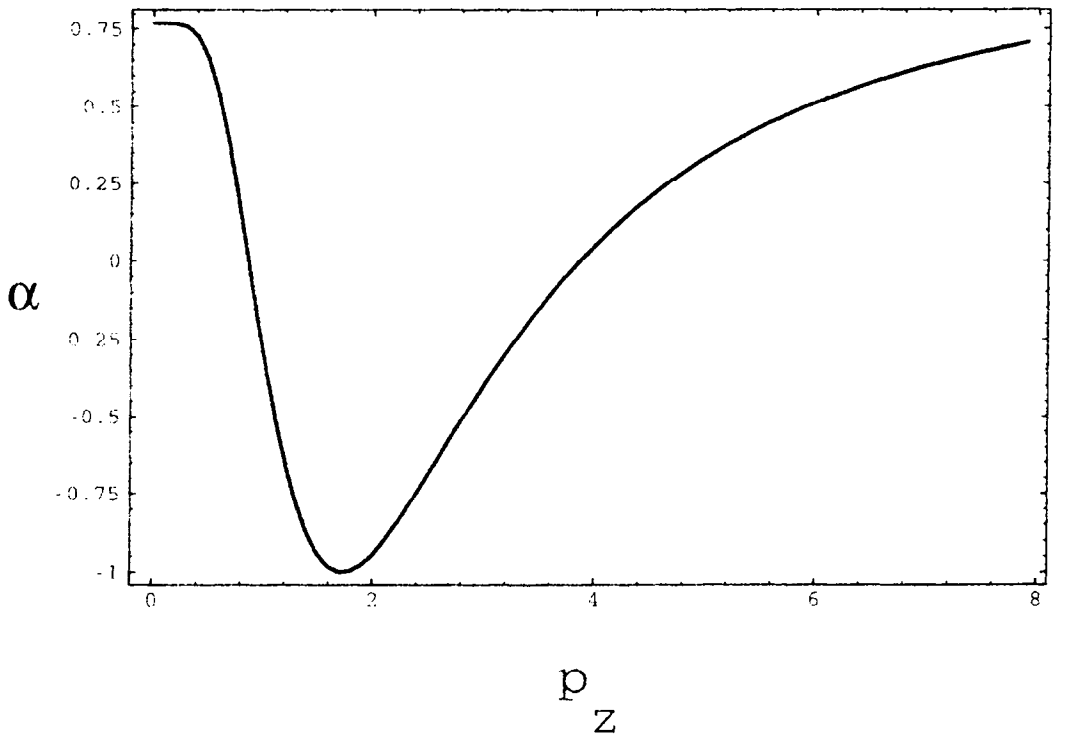

Fig. 4. Analytical estimation for the index α as function of p_z, for $A_0 = 0.05$, $k = \omega = 1$.

4. SEQUENCES OF BIFURCATION-RECONNECTIONS

In this section, we will analyze the sequences of bifurcation-reconnections that characterize the generation (annihilation) of resonances as the parameter p_z decrease (increase). First one deals with the generic case of any resonant chain, and then we will analyze the case of the resonance [2:1].

In all cases, the sequence that characterizes the generation (annihilation) process actually changes the phase space and destroys the regular acceleration of particles. Some of the most important resonances are indicated in Fig. 3(a), but the most dangerous resonance is the [2:1] because the elliptic point of the nonpendular island lost stability during the process as we shall see later.

4.1 Generic case

Two aspects are important in the generation of generic resonances inside the nonpendular island: there are no windows of instability and the pattern of bifurcations is typical. The sequence of bifurcations as p_z decreases is as follows. The generic case will be analyzed as a function of a decreasing p_z. At the beginning, there is the nonpendular island and the ring of reconnection that is the minimum of frequency. As the reconnection ring takes on a rational value, two sets of pairs of elliptic-hyperbolic points are bifurcated via a tangent inverse process. After this, by reconnection, two secondary resonant chains are formed and both of them migrate, the internal one towards the elliptic point and the external towards the boundary of the nonpendular island. The internal resonance vanishes in the elliptic point according to a typical bifurcation [13] and the external one crosses the boundary becoming a primary resonance.

We will illustrate this situation with the help of a sequence of Poincaré plots for the case of resonance [1:5]. The Hamiltonian in eqn (3) is integrated for $\omega = k = 1$, $A_0 = 0.125$ and various values of p_z. In Fig. 5(a), with $p_z = 0.42$, is shown the nonpendular island before any bifurcation. In Fig. 5(b), where $p_z = 0.41$, is presented the first set of coupled elliptic-hyperbolic points that was produced via tangent inverse bifurcations. In Fig. 5(c), where $p_z = 0.4025$, the first and the second pairs of elliptic and hyperbolic points are shown. The asymmetric behavior in the creation of the two sets of hyperbolic-elliptic points is credited to the shape of the curve of the frequency inside the nonpendular island that is not parabolic; see Fig. 2. In Fig. 5(d), where $p_z = 0.40$, the reconnection process is accomplished. And finally in Fig. 5(e), where $p_z = 0.37$, the internal resonance has already vanished close to the elliptic point of the nonpendular island according to a typical bifurcation [13]. The external resonance has crossed the boundary of the nonpendular island.

4.2 Case of resonance [2:1]

The process involving the resonance [2:1] is special because a window of instability is formed during this process, i.e. the elliptic fixed point of the nonpendular island becomes hyperbolic during the process. The sequence of bifurcations and the window of instability will be illustrated with the help of Poincaré plots. We integrate the Hamiltonian of eqn (3) for $\omega = k = 1$, $A_0 = 0.1$ and some convenient values of p_z.

The process involving the resonance [2:1] will be analysed, as p_z is increased, the annihilation process. Fig. 6(a), where $p_z = 1.58$, shows the resonance [2:1] close to the nonpendular island. Fig. 6(b) corresponds to the same value of p_z, a zoom of the first island is done. The next step corresponds to the period-doubling bifurcation of the nonpendular island that produces new elliptic and hyperbolic points; the two elliptic points of the nonpendular island collide via tangent inverse bifurcation with the hyperbolic points of the resonance [2:1]. These bifurcations were shown in a previous work [6]; the difference is that in that

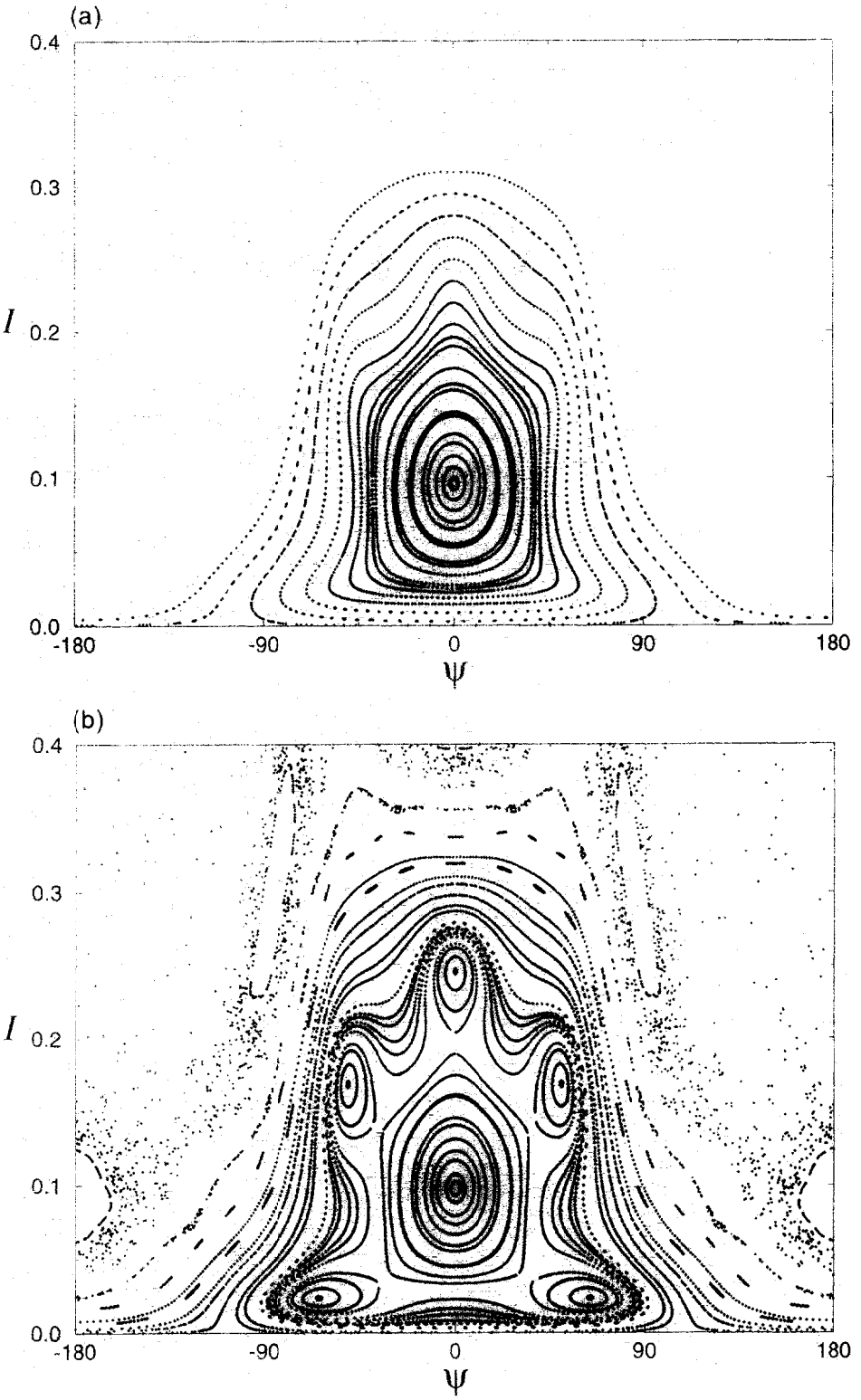

Fig. 5. Caption on p. 388.

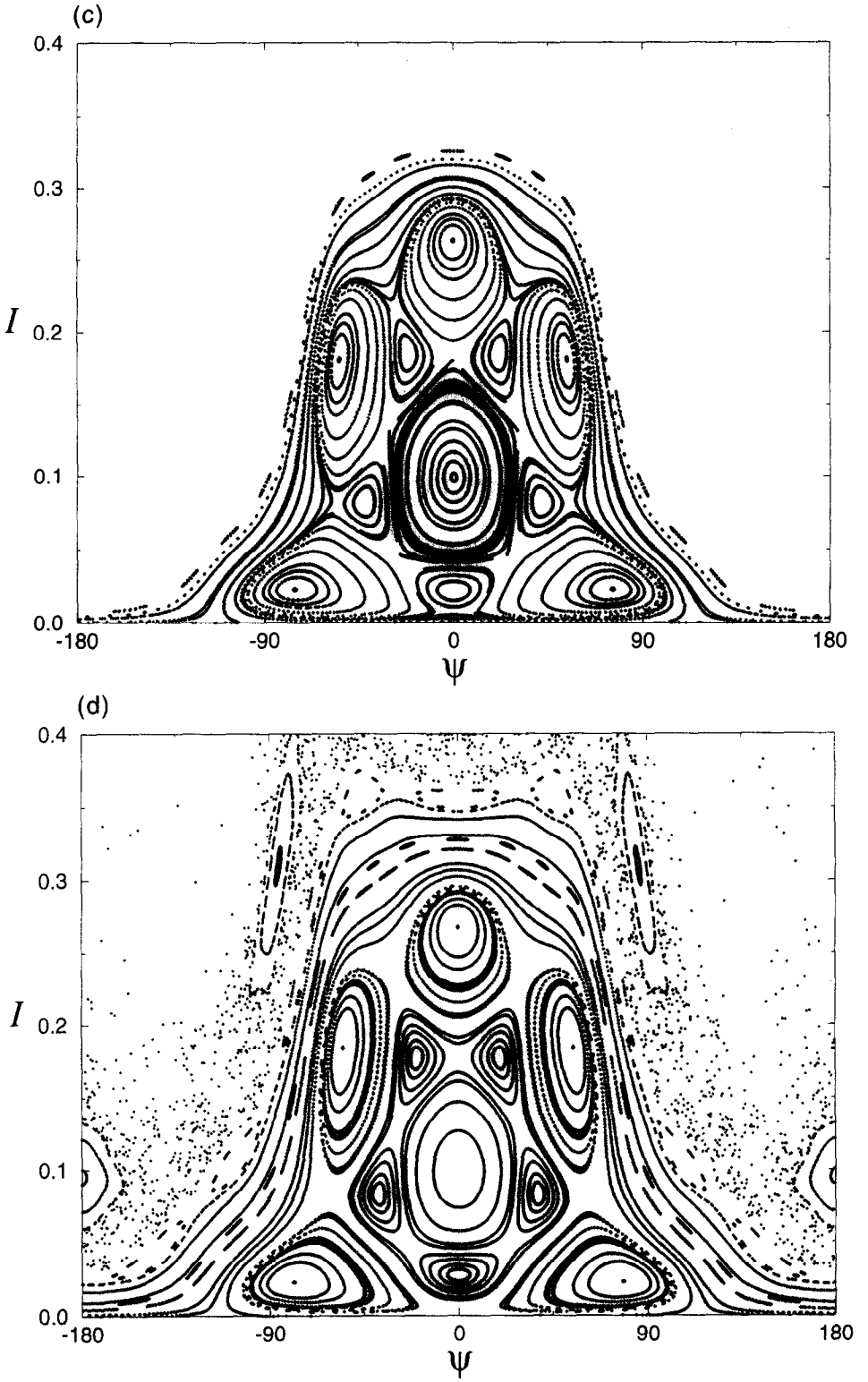

Fig. 5. Caption overleaf.

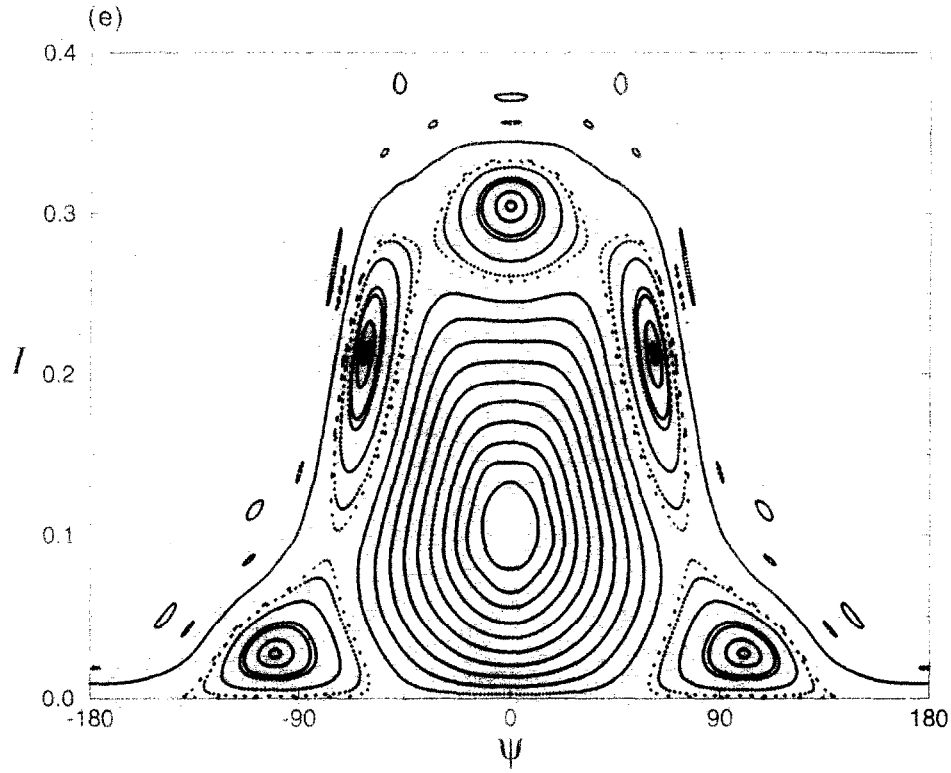

Fig. 5. Bifurcation-reconnection process inside the nonpendular island. $A_0 = 0.125$, $k = \omega = 1$. (a) $p_z = 0.42$, the nonpendular island; (b) $p_z = 0.41$, the first set of elliptic and hyperbolic points; (c) $p_z = 0.4025$, the first and the second sets of elliptic and hyperbolic points; (d) $p_z = 0.40$, two chains produced after the reconnection; (e) $p_z = 0.37$, the external resonance crosses the nonpendular boundary and the internal one suffers bifurcation.

paper we were interested in the transition to chaos, and the bifurcation of the nonpendular island was done by increasing the amplitude of the wave A_0. Figure 6(c), where $p_z = 1.7$, shows the remaining fixed points, the hyperbolic of the nonpendular island and the two elliptics of the resonance [2:1]. Finally in Fig. 6(d), where $p_z = 1.85$, we recover the nonpendular island after an inverse doubling bifurcation.

Figure 7 shows the stability diagram for the central fixed point of the nonpendular island. The interval at which the point is hyperbolic, the instability interval, is below the long dashed line and the interval at which the point is elliptic is above this line. The diagram has on the vertical axis the stability index α and on the horizontal axis the parameter p_z. The Newton–Raphson algorithm reveals that the central fixed point of the nonpendular island is not stable for $1.6 < p_z < 1.84$.

5. FINAL REMARKS

A global analysis of the origin of the resonant chains of the system is accomplished and it is concluded that all the primary resonant chains can be viewed as being originated by a sequence of bifurcations and reconnections from a ring placed around the elliptic fixed point of the nonpendular island. This topic suggests one question to be posed in the context of nonlinear Hamiltonian systems: in what circumstances is it possible to describe the complex variety of resonances of a generic Hamiltonian as an unfold of bifurcations from a single resonant island?

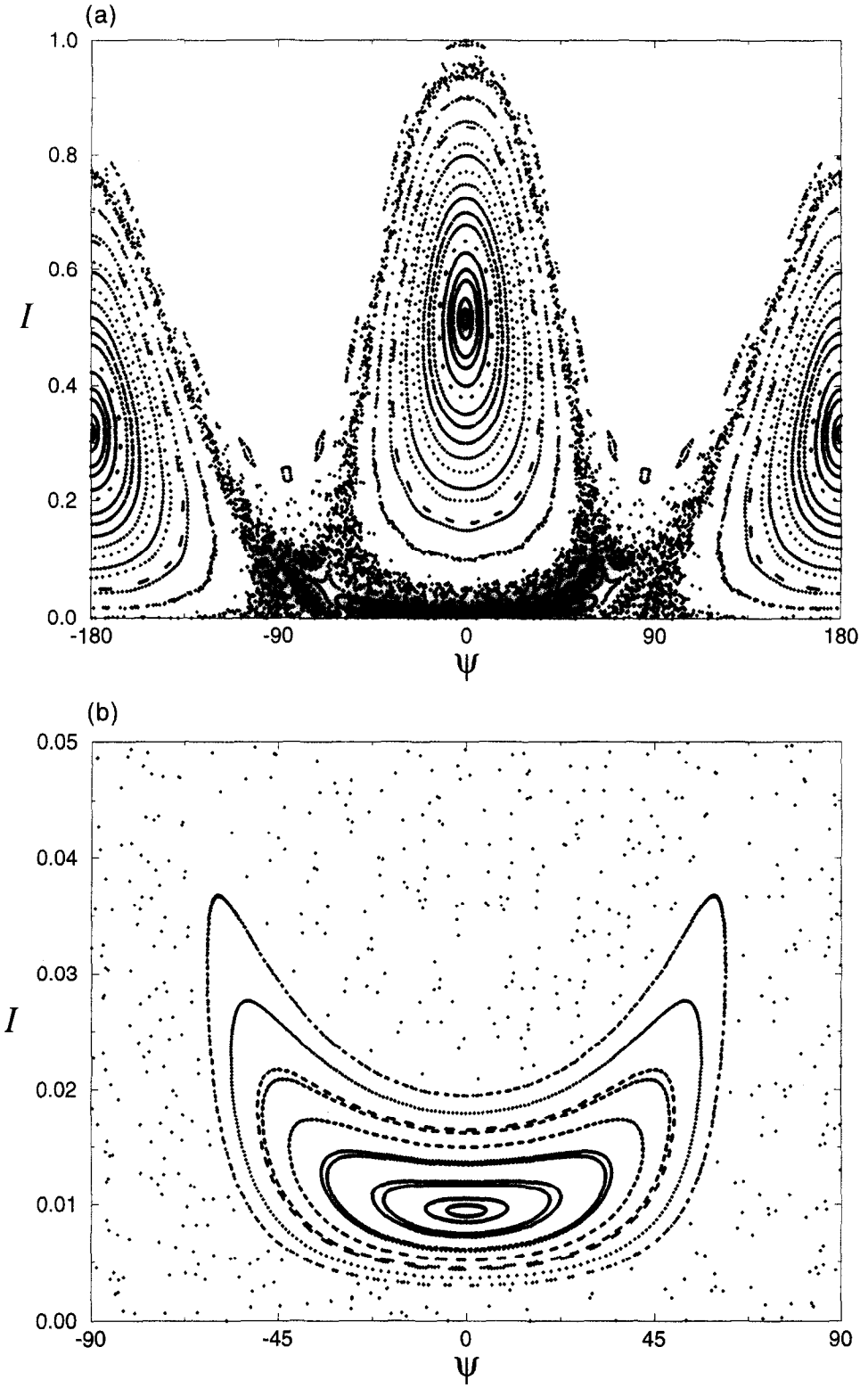

Fig. 6. Caption overleaf.

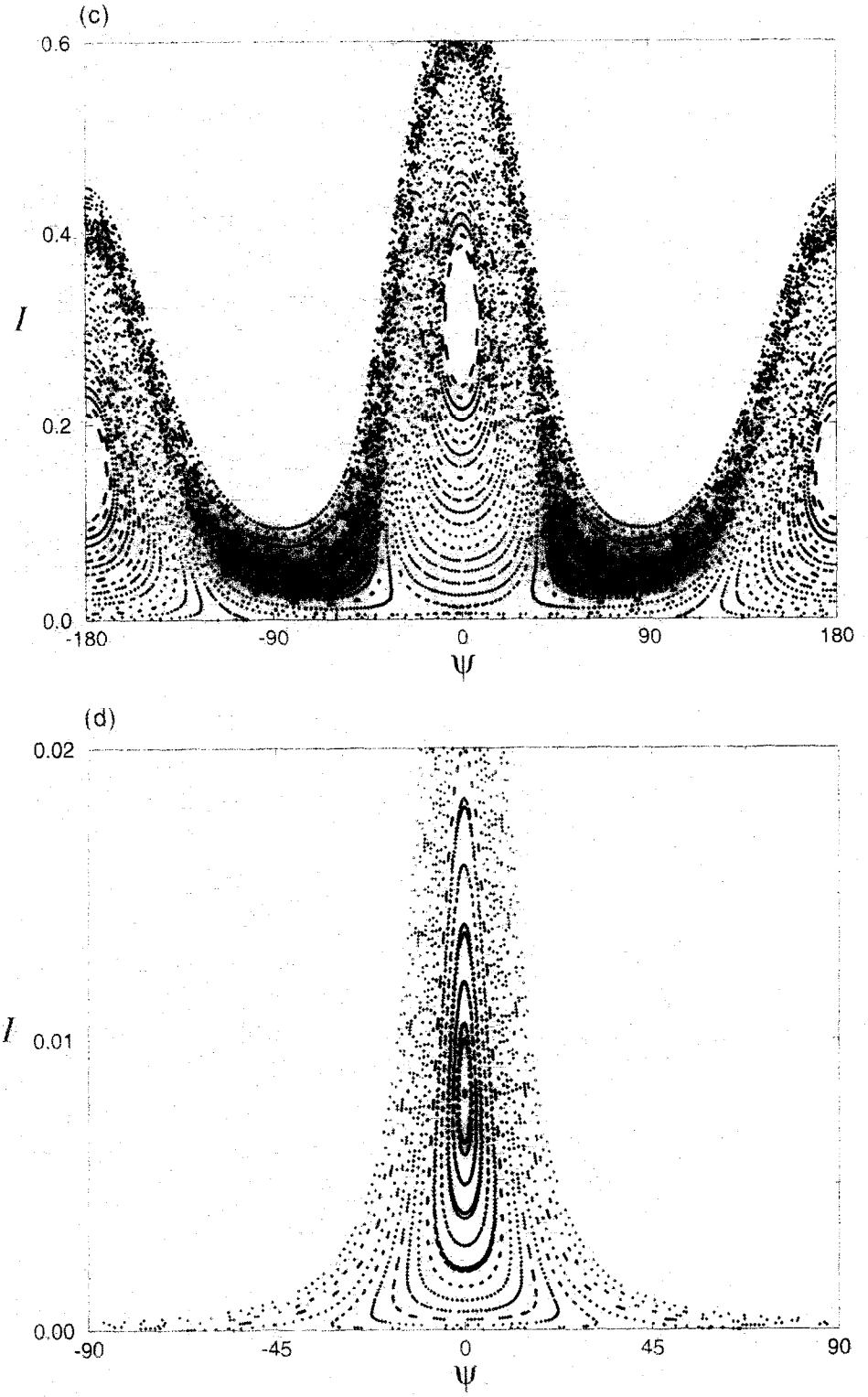

Fig. 6. Poincaré plot showing a sequence of bifurcations involving nonpendular island and the resonance [2:1]. (a) $p_x = 1.58$, the resonance [2:1] and the nonpendular island; (b) zoom of the previous figure showing the nonpendular island; (c) $p_x = 1.7$, the hyperbolic point of the nonpendular island and the two elliptic points of the resonance [2:1]; (d) $p_x = 1.85$, the nonpendular island after the annihilation of the resonance [2:1].

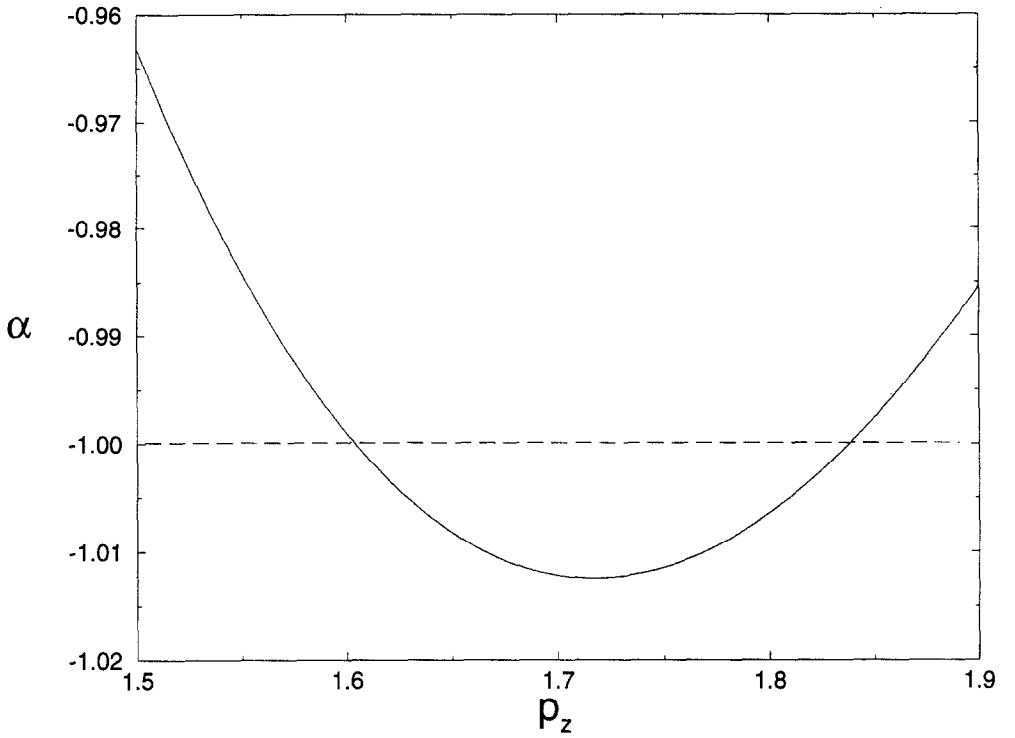

Fig. 7. Stability diagrams showing the index α of the central fixed point of the nonpendular island vs the value of p_z. Below the long dashed line instability is characterized.

The method of effective potential for the local Hamiltonian that describe the nonpendular island is used in order to estimate its frequency, which is nonmonotonic along the radius of the island. A simulation and a theoretical analysis is done for the frequency of the elliptical point of the nonpendular island as the parameter p_z varies. An estimation of critical values of p_z that generate resonances is done; these values disturb a regular acceleration of particles and must be evicted in a experimental system.

We can describe the complex topology of this system from the unfold of resonances of the nonpendular island. In the limit of parameter p_z infinite, the system is integrable and the nonpendular island occupies all the phase space. The generation of resonances from the nonpendular island is a stable process unless to the resonance [2:1]. In the generic situation as p_z decreases the sequence of bifurcation-reconnections is as follows: a set of pairs of elliptic-hyperbolic points is generated by tangent inverse bifurcation close to the extremum of frequency (reconnection ring) and suffer reconnection setting up a pair of resonance chains; the internal resonance collapses into the elliptical point as the external one crosses the nonpendular boundary becoming a primary resonance. The chains produced in the nonpendular island establish all the primary chains of the Hamiltonian phase space.

Acknowledgements—We acknowledge partial support by CNPq, CAPES and FINEP (Brazil). Part of the numerical work was performed on the Cray YMP-2E at the Supercomputing Center of the Universidade Federal do Rio Grande do Sul. G. Corso and R. Pakter acknowledge the support of the Instituto de Física, Universidade de São Paulo, Brazil, where part of this work was performed.

REFERENCES

1. Van der Weele, J. P., Vakering, T. D., Chapel, H. W. and Post, T., *Physica A*, 1988, **153,** 283.
2. Oda, G. A. and Caldas, I. L., *Chaos, Solitons & Fractals*, 1995, **5,** 15.

3. Davidson, R. C., Yang, Y.-T. and Aamodt, R. E., *J. Plasma Phys.*, 1989, **41**, 405.
4. Farina, D. and Pozzoli, R., *Phys. Rev. A*, 1992, **45**, R575.
5. Corso, G. and Rizzato, F. B., *Phys. Rev. E*, 1995, **52**, 3591.
6. Corso, G. and Rizzato, F. B., *Physica D*, 1995, **80**, 296.
7. Winter, O. C. and Murray, C. D., *Astronom. Astrophys.*, 1996, **319**, 290.
8. Pakter, R., Schneider, R. S. and Rizzato, F. B., *Phys. Rev. E*, 1994, **49**, 1594.
9. Pakter, R. and Corso, G., *Phys. Plasmas*, 1995, **2**, 4312.
10. Brunnet, L. G., Corso, G. and Rizzato, F. B., *Phys. Lett. A*, submitted.
11. Lichtenberg, A. J. and Lieberman, M. A., *Regular and Stochastic Motion*, Springer, Berlin, 1983.
12. Polymilis, G. and Hyzanidis, K., *Phys. Rev. E*, 1993, **47**, 4381.
13. Arrowsmith, D. K. and Place, C. M., *An Introduction to Dynamical Systems*, Cambridge University Press, Cambridge, 1990.
14. Corso, G. and Rizzato, F. B., *J. Plasma Phys.*, 1993, **49**, 425.